Time-Dependent Density-Functional Studies of the D_2 Coulomb Explosion†

Ester Livshits and Roi Baer*

Department of Physical Chemistry and the Lise Meitner Minerva-Center for Quantum Chemistry, the Hebrew University of Jerusalem, Jerusalem 91904 Israel

Received: January 4, 2006; In Final Form: March 15, 2006

Real-time first principle simulations are presented of the D_2 Coulomb explosion dynamics detonated by exposure to very intense few-cycle laser pulse. Three approximate functionals within the time-dependent density functional theory (TDDFT) functionals are examined for describing the electron dynamics, including time-dependent Hartree−Fock theory. Nuclei are treated classically with quantum corrections. The calculated results are sensitive to the underlying electronic structure theory, showing too narrow kinetic energy distribution peaked at too high kinetic energy when compared with recent experimental results (*Phys. Rev. Lett.* **2003**, *91*, 093002). Experiment also shows a low energy peak which is not seen in the present calculation. We conclude that while Ehrenfest−adiabatic−TDDFT can qualitatively account for the dynamics, it requires further development, probably beyond the adiabatic approximation, to be quantitative.

I. Introduction

Time-dependent density functional theory[1] (TDDFT) is emerging as a useful tool for simulating the dynamics of electrons in molecules.[2−28] Combined with the Ehrenfest molecular dynamics approach,[20,29−31] one obtains a potentially powerful method for studying processes under strong electronic excitations. Yet, due to lack of appropriate experiments, the theory has not been sufficiently well tested. In this paper we discuss experimental results that can be used to study combined electron−nuclear dynamics under strong laser field conditions. We focus on Coulomb explosion experiments[32−38] detonated by short and intense laser pulses, as recently reported.[33] The pulses rapidly double-ionize the molecules, shattering them into positively charged fragments which then recede under the influence of the Coulomb repulsion. We simulate the experiment in real time using a first principles approach (i.e., no adjustable parameters) founded on two major approximations. The nuclear dynamics is treated using classical mechanics, with the electron−nuclear force derived from the instantaneous mean electron−nuclear Coulomb potential. We also correct classical dynamics, to some degree, by sampling the initial conditions from an approximate (i.e., Gaussian) Wigner distribution corresponding to the initial vibrational ground-state. The second approximation involves the description of the electron dynamics within approximate time-dependent density functionals. One benefit of the approximation is that it is essentially from first principles and includes no prejudice as to the mechanism of the ionization and the nuclear motion.

We chose to treat the simplest case, that of an ultrashort (<10 fs) very intense (>10^{15} W cm^{-2}) infrared laser pulse applied to a small molecule, such as D_2. This set of conditions are reported in the recent experiments of Legaré et al.[33] This system is a prototype for developing methods to study the fusion induced by Coulomb explosion in large deuterium clusters.[39,40] In this regime of pulse strength and pulse duration, it is expected that nonsequential double ionization is a major dissociation channel.[33,41,42] Furthermore, in such experiments, the short time it takes to ionize the electrons is expected to suppress many of the intricate electron−nuclear coupling effects, as was shown[43] for 5 fs pulses in the case of H_2^+. Despite this apparent simplification, we find that considerable nuclear motion exists (D−D distance extending by as much as $3a_0$, depending on initial conditions) during the ionization process. This makes the present experimental setup a sensitive probe of the resulting electron−nuclear dynamics, enough to compare and differentiate between time-dependent density functional theories.

In this work, we examine three TDDFT functionals. The first is the simplest TDDFT approach, the adiabatic local density approximation (ALDA). The second functional is the time-dependent Hartree−Fock (TDHF). For two electrons in an initial singlet state TDHF is a density functional theory. There are two issues which account for the difference between these approaches: electron correlation and self-interaction. ALDA accounts (approximately) for electron correlation. Yet, it suffers from self-interaction. TDHF ignores correlation altogether, but has no spurious self-interaction. A recent study of the exact exchange-correlation potential in a one-dimensional model for the strong field ionization of the Helium atom[44] revealed that derivative discontinuities[45] have an important role in a correct description of the observed nonsequential double ionization.[42,46] However, ALDA cannot account for derivative discontinuities. This is mainly because ALDA includes spurious self-interaction. As noted above, TDHF does not suffer from self-interaction. Yet, since it completely neglects electron correlation, it has been shown to lead to incorrect results of nonsequential ionization as well as overestimating the tunneling rate under strong laser intensities.[47] This prompts us to use a third functional, the recently developed density functional, the Baer−Neuhauser[48] $\gamma = 1$ (BN1). In a time-dependent context, we call it the adiabatic BN1 (ABN1) functional. This functional does not suffer from long-range self-repulsion and it incorporates ground-state correlation effects similar to that of ALDA.

The final conclusion of this paper is that while the experiment is sensitive to the underlying electron dynamics model, the

† Part of the "Chava Lifshitz Memorial Issue".

* To whom correspondence should be addressed. Email: roi.baer@huji.ac.il.

10.1021/jp0600460 CCC: $33.50
Published on Web 04/20/2006

functionals we try do not successfully account for the experimental results. We attribute this failure to the fact that the calculations exhibit much too high double ionization rate. This is somewhat similar to the case of strong field ionization of He.[47] However, the failure has other sources, as discussed in the summary.

We first describe the theoretical and numerical method in section II. We then present, in section III, the results of an archetypal run using TDDFT and the kinetic energy distribution of the exploding nuclei calculated within the adiabatic local density approximation (ALDA). In section III.B, we present the results of the simulation with two additional TDDFT functionals. A discussion of the results is given in 0.

II. Theory

A. Ehrenfest Molecular Dynamics within TD-ALDA. An ab initio study of the laser−molecule interaction under fully realistic conditions is still beyond our reach. Our approach therefore starts by an approximation that the N_N nuclei of the molecule can be treated classically. The total force on nucleus I ($I = 1, ..., N_N$) is composed of the mutual Coulombic repulsion, the *average* electronic attraction, and any external homogeneous electric field **E** (due to a laser or static field):

$$\mathbf{F}_I[\{\mathbf{R}\},\mathbf{E},n] = \sum_{J\neq I}\frac{Z_I Z_J}{|\mathbf{R}_J-\mathbf{R}_I|^3}(\mathbf{R}_J-\mathbf{R}_I) - \int n(\mathbf{r})\frac{Z_I}{|\mathbf{r}-\mathbf{R}_I|^3}(\mathbf{r}-\mathbf{R}_I)\,\mathrm{d}^3r + Z_I\mathbf{E} \quad (2.1)$$

where $n(\mathbf{r})$ is the electron density at point $\mathbf{r}$ and $\mathbf{R}_I$, Z_I are, respectively, the position and charge of nuclei I. In all formulas we use atomic units, $e^2/4\pi\epsilon_0 = 1$, $\hbar = h/2\pi = 1$, and $\mu_e = 1$, where e, μ_e, ϵ_0, and h are respectively the electron charge, mass, the vacuum permittivity, and Planck's constant.

The Born−Oppenheimer ground-state potential surface is computed using the local density and local spin-density approximations (LDA and LSDA).[49,50] We now briefly outline the LSDA. LDA is obtained by constraining the equality of spin-up and spin-down densities. The electronic density is assumed to be represented by Kohn−Sham (KS) orbitals $\psi_{n,s}(\mathbf{r})$, $n = 1, ..., N_e/2$ (N_e is the number of electrons, assumed to be even), and $s = \uparrow,\downarrow$ designates the spin of the orbital:

$$n_s(\mathbf{r}) = \sum_{n=1}^{N_e/2}|\psi_{n,s}(\mathbf{r})|^2, \quad s = \uparrow,\downarrow \quad (2.2)$$

The total electronic density is the sum of spin densities:

$$n(\mathbf{r}) = n_\uparrow(\mathbf{r}) + n_\downarrow(\mathbf{r}) \quad (2.3)$$

The orbitals are obtained from the KS equation:[49]

$$-\frac{1}{2}\nabla^2\psi_{n,s} + v_s(\mathbf{r})\psi_{n,s} = \epsilon_{n,s}\psi_{n,s} \quad (2.4)$$

Here and throughout the paper atomic units are used. Where the spin-polarized effective potential $v_s(\mathbf{r})$ depends on the density:

$$v_s[n;\{\mathbf{R}\};\mathbf{E}](\mathbf{r}) = v_H[n](\mathbf{r}) + v_+(\mathbf{r};\{\mathbf{R}\}) - \mathbf{E}\cdot\mathbf{r} + v_{\mathrm{XC}}[n](\mathbf{r}), \quad (2.5)$$

where $v_+(\mathbf{r})$ is the potential energy due to interaction with the nuclei:

$$v_+(\mathbf{r};\{\mathbf{R}\}) = -\sum_{I=1}^{N_N}\frac{Z_I}{|\mathbf{r}-\mathbf{R}_I|} \quad (2.6)$$

$v_H[n](\mathbf{r})$ in eq 2.5 is the repulsive electrostatic potential energy due to interaction of an electron with the electronic charge density $n(\mathbf{r}) = n_\uparrow(\mathbf{r}) + n_\downarrow(\mathbf{r})$:

$$v_H[n](\mathbf{r}) = \int\frac{n(\mathbf{r}')}{|\mathbf{r}-\mathbf{r}'|}\,\mathrm{d}^3r' \quad (2.7)$$

Finally, the exchange-correlation (XC) potential is given by

$$v_{\mathrm{XC}}[n](\mathbf{r}) = \frac{d}{dn}[n(\mathbf{r})\epsilon_{\mathrm{XC}}(n(\mathbf{r}))] \quad (2.8)$$

where $\epsilon_{\mathrm{XC}}(n) = \epsilon_{\mathrm{X}}(n) + \epsilon_{\mathrm{C}}(n)$ is the XC energy per particle of the homogeneous electron gas (we use for ϵ_{X} and ϵ_{C} the parametrizations of ref 51). We have also tested other XC potentials, as described below. Equation 2.4 must be solved self-consistently with eqs 2.2 and 2.5. Once this is achieved, the Born−Oppenheimer energy curve $V_{\mathrm{ad}}(\{\mathbf{R}\})$. In the present case, the molecule studied is D_2 and the potential curve only depends on the distance between the two nuclei, thus we denote it as $V_{\mathrm{ad}}(R)$.

Next, we discuss the dynamics of the nuclei and the electrons in the molecule under the influence of a homogeneous electric field pulse of duration T and frequency ω given by

$$\mathbf{E}(t) = \hat{\mathrm{z}}E_0\cos(\omega t)\times\begin{cases}\sin^2\left(\frac{\pi t}{T}\right) & t < T\\ 0 & \text{otherwise}\end{cases} \quad (2.9)$$

In the present calculation we used $E_0 = 0.28\ E_h$, $T = 17.2\ fs$ and $\omega = 0.056\ E_h\hbar^{-1}$ in accordance with one of the experiments of Legaré et al.[33]

To compute the ensuing dynamics, we use the Ehrenfest molecular dynamics approach,[52,53] leading to the following equation of motion for the nuclei:

$$M_I\ddot{\mathbf{R}}_I(t) = \mathbf{F}_I[\{\mathbf{R}(t)\}, \mathbf{E}(t), n(t)] \quad (2.10)$$

We have also added corrections for quantum effects, by sampling the initial conditions for this equation from the ground-state vibrational wave function of Deuterium.

The time dependent electron density $n(\mathbf{r},t)$ is calculated using time-dependent density functional theory, in the adiabatic local spin-density approximation.[1] This is done by solving the time-dependent Kohn−Sham equations:

$$i\frac{\partial\psi_{n,s}(\mathbf{r},t)}{\partial t} = -\frac{1}{2}\nabla^2\psi_{n,s}(\mathbf{r},t) + v_s[n(t), \{\mathbf{R}(t)\}, \mathbf{E}(t)](\mathbf{r})\psi_{n,s}(\mathbf{r},t), \quad (2.11)$$

where v_s is given in eq 2.5. The real-time approach to ALDA has been shown to be a useful tool for analyzing a variety of molecular electron dynamics problems.[2,7,54−57] Recently, new methods were developed for including nonadiabatic[58] effects in the exchange correlation effects.[59−62]

Ehrenfest molecular dynamics (EMD) approach was evaluated by Uhlmann et al.[63] for a setting similar to ours. They studied H_2^+ ionization by strong electric pulse, for which full quantum mechanical results exits.[64] One conclusion of their study was that EMD is impressively accurate for strong laser fields, once

TABLE 1: Parameters A_γ^i in Eq 2.15 for Two Values of γ

i	$\gamma = 1a_0^{-1}$	$\gamma = 0.8a_0^{-1}$
0	5.37708359	4.32761343
1	−2.22492999	−1.79674968
2	0.14024288	0.18079773
3	7.09028096	2.53111942
4	15.67508416	23.05256819

the electron is properly described by a large enough Gaussian basis set. In our study, we use a grid for describing the electronic wave function and we do not expect any such basis set problem.

B. Time-Dependent Hartree−Fock Calculations. The TDDFT method described in the previous section can be easily modified to accommodate the time-dependent Hartree−Fock calculations. One need only replace the exchange correlation potential of eq 2.8 by the Hartree−Fock exact exchange operator, which in the present 2-electron singlet context is nothing more than the potential:

$$v_x(\mathbf{r}) = -\frac{1}{2}v_H(\mathbf{r}) \tag{2.12}$$

C. ABN1 − A Functional Without Long-Range Repulsion. The self-repulsion in LDA prevents the functional from describing correctly the derivative discontinuities in the exchange correlation potential.[65] This problem also extends to time-dependent ALDA and was recently shown to have an important role in correct description of ionization processes in helium.[44] The time-dependent Hartree−Fock method does not suffer from this drawback. However, it completely neglects correlation. Recently a DFT functional was developed that does not have long range self-repulsion, accounting correctly for the asymptotic potential and for derivative discontinuity.[48] We refer to this functional as ABN1.

The functional is described here, referring the reader to ref 48 for explanation of the method. The XC potential of the ABN1 functional is given by

$$v_{XC}^\gamma[n](\mathbf{r}) = \frac{d}{dn}[n(\mathbf{r})\epsilon_{XC}^\gamma(n(\mathbf{r}))] + v_X^\gamma(\mathbf{r}), \tag{2.13}$$

where the explicit nonlocal exchange (which for 2 electrons takes the form of a potential) is

$$v_X^\gamma(\mathbf{r}) = -\frac{1}{2}\int \frac{n(\mathbf{r}')e^{-\gamma|\mathbf{r}-\mathbf{r}'|}}{|\mathbf{r}-\mathbf{r}'|}\,d^3r' \tag{2.14}$$

Here γ is a parameter of the functional, which assumes the value $\gamma = 1a_0^{-1}$. Furthermore, in eq 2.13 $\epsilon_{XC}^\gamma(n) = \epsilon_X^\gamma(n) + \eta_\gamma(\gamma r_s)\epsilon_C(n)$, where $\epsilon_c(n)$ is the LDA correlation energy per particle[51] and the factor $\eta_\gamma(\gamma r_s)$ ($r_s^3 = 3na_0^3/4\pi$ is the Wigner-Seitz radius) is given by

$$\eta_\gamma(x) = \frac{C}{A_\gamma^0 + A_\gamma^1 x + x^2} + \frac{B}{A_\gamma^2 x^3 + A_\gamma^3 x^{3/2} + (A_\gamma^4 - \ln x)x} \tag{2.15}$$

This form for η_γ and the value of the parameters, $C = 1.6976$, $B = 12.8$ ensures correct asymptotic $r_s \to \infty$ and $r_s \to 0$ limits. The low-density behavior of η is determined from an analogue of Wigner's theory for low-density gas of particles interacting by a screened Coulomb potential[66] and the high-density limit, is based on correlation energy estimates given in ref 67. The parameters A_γ^i, $i = 0, ..., 4$ are determined using Monte Carlo calculations, as described in ref 48. For $\gamma = 1a_0^{-1}$ and $0.8a_0^{-1}$ they are given in Table 1. Finally, ϵ_X^γ is the local exchange energy of a screened Coulomb interacting gas of particles, based on ref 68:

$$\tilde{\epsilon}_X^\gamma[n] = -\frac{3k_F}{4\pi}H\left(\frac{\gamma}{k_F}\right), \tag{2.16}$$

where k_F is the Fermi momentum of the HEG, $k_F = (3\pi^2 n)^{1/3}$ and:

$$H(q) = 1 - \frac{q^2}{6} - \frac{4q}{3}\tan^{-1}\left(\frac{2}{q}\right) + \frac{q^2}{24}(12 + q^2)\ln\left(\frac{4}{q^2} + 1\right) \tag{2.17}$$

We have recently proved[69] that γ can take values from a continuous range of values. Thus, while the choice of γ is arbitrary, taking $\gamma = 1$ or $0.8a_0$ hardly affects the results.

D. Implementation Issues and Parameters. The Kohn Sham (or TDHF) eqs 2.11 are implemented using a plane-waves basis[70,71] and pseudopotentials,[72] with cutoff energy of 30 E_h, a cubic cell size of size $36a_0$. The calculation consists of a single orbital, i.e., closed shell zero spin.[73] A fifth-order adaptive Runge−Kutta method[74] was used to evolve the electron density in time. The position and velocity of the nuclei (eq 2.10), was updated using the velocity-Verlet method, with time step of $\Delta t = 0.5\hbar E_h^{-1}$. Typically, the electronic time-step is much lower (by a factor of about 20) than the nuclear time-step.

To remove the outgoing electron flux, which is rendered "ionized", an absorbing complex potential[75] is placed in the asymptotic directions. The form of the imaginary potential is as follows: $W(\mathbf{r}) = w(x) + w(y) + w(z)$, with $w(x)$ defined by

$$w(x) = \begin{cases} -(1+i)\eta(|x| - a)^n & a \le |x| \le L/2 \\ 0 & \text{otherwise} \end{cases} \tag{2.18}$$

The parameters are given by: $n = 3$, $a = 7a_0$, and $\eta = 3.8 \times 10^{-4}E_h$.

We have made extensive checks that the results shown are well converged, in space by increasing box size and grid-point density, in time by checking the propagator time-step and in terms of the absorbing potential parameters.

III. ALDA Results

A. Archetypal Run. Let us first study in detail the results from a single case considered "Archetypal". The archetype set of initial conditions describes a molecule aligned along the electric field polarization (z axis); the nuclei start with zero initial velocity at the separation R_{eq} corresponding to the minimum of the adiabatic potential surface V_{ad}. The electrons start from their Kohn−Sham ground-state orbitals at this nuclear configuration. The field $\mathbf{E}(t) = E(t)\hat{\mathbf{z}}$ is then switched on and the resulting dynamics is followed numerically.

At $t = 0$ the field is turned on and starts to shake the electrons, exciting and subsequently rapidly ionizing them. We monitor the electron flux through a plane situated at $z = 6a_0$ (parallel to the $x-y$ plane) as a function of time. This rate is shown in Figure 1a. The flux is highly correlated with the electric field. Ionization starts at $t \approx 3$ fs and ends at $t = 9$ fs when most electronic density is far enough from the nuclei (in practice most flux reaching a distance larger than $8a_0$ is absorbed by the complex potential). An interesting feature is the small amount of recollision, i.e., negative flux through the plane, meaning that the high harmonic generation yield is expected to be small. Another noticeable effect is the small sharp peaks in the flux at $t = 7.7$ to $8\hbar E_h^{-1}$. These peaks occur when the D−D distance

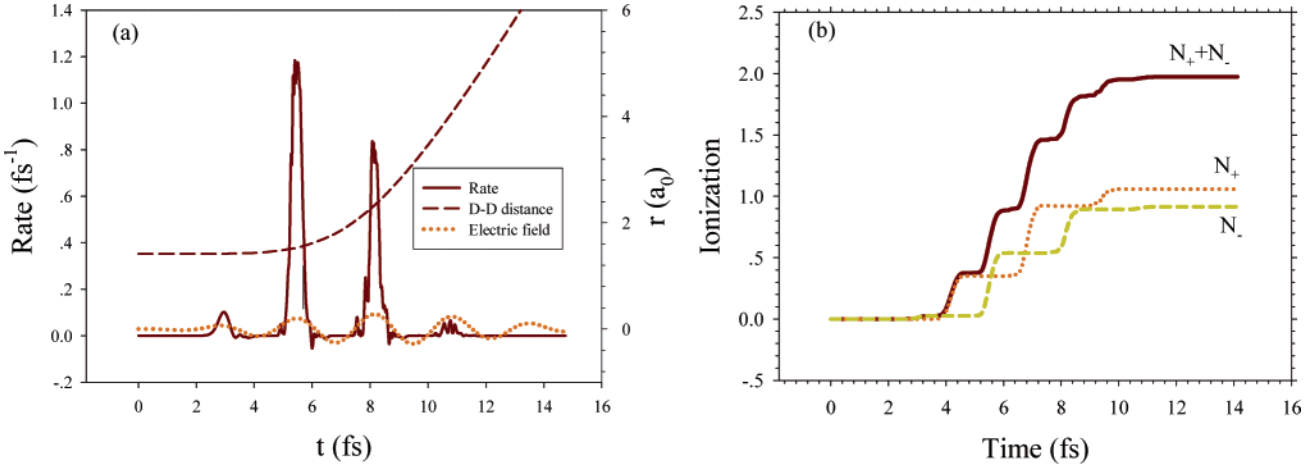

Figure 1. (a) Rate of electron crossing a plane perpendicular to the *z*-axis at $z = 6a_0$ as a function of time (solid). Also shown, are the electric field (dotted) and the D−D distance (dashed). (b) Ionization vs time. About 99% of ionization is achieved in the *z* directions. Results are for the archetypal run.

is around $2a_0$, and they are probably due to resonances that enhance ionization.

In Figure 1 (right panel), we show the integrated flux in the positive and negative directions of the *z* axis. The results for the two channels will depend sensitively on the phase of the laser. However, the sum of the two channels will not.

Because of the short time duration needed to achieve full ionization, one wonders if the nuclei have enough time to move at all. The simplest approximation then would be to assume they are stationary during the ionization. This would give an upper estimate of the final kinetic energy per nuclei (at the bond distance of $R = 1.42a_0$) equal to the Coulomb repulsion energy $E_{rep} \approx 9.6$ eV. The Legaré et al. experiment[33] shows however that the final kinetic energy of the deuterium nuclei is around 6.5 eV. This means that the nuclei moved considerably during the ionization process. Indeed, under the conditions of the experiment, the situation is radically different from ordinary chemical conditions. Once a large part of the electronic cloud is torn away from the molecule, the force of repulsion between the nuclei is very strong. We define an *effective* force of repulsion between the deuterium nuclei using the computed relative acceleration

$$F_{eff} = \mu\ddot{R} \tag{3.1}$$

where μ is the reduced mass. This force, as a function of nuclear distance is compared with the bare Coulomb force of repulsion in Figure 2c. In this calculation Since the force is computed for a pair of atoms starting in the equilibrium point, it is zero at the initial bond length. As the laser is switched on, the force is seen to be completely repulsive. At distances close to the ground-state minimum this is no surprise, the electric field initially excites electrons to the repulsive excited-state potentials of D_2. As the field strengthens the amount of excitation quickly dominates (before ionization sets in) and the force between the nuclei becomes even more repulsive. This phenomenon is a type of "bond softening", reminiscent observed in H_2^+,[76] for weaker, longer (and optical) pulses. The effective force is repulsive (positive) throughout the Coulomb explosion process. It contains oscillations which are due to the oscillating nature of the electronic motion, in response to the electric field. In Figure 2c, we also see a clear correlation between the repulsive nature of the force and the instantaneous value of the electric field. It seems that the repulsive force increases when the electric field intensity is maximal since then electrons are effectively pushed out of the inter-bond region. For example, in the D−D distance range of $2.3a_0$ and $2.5a_0$, the effective force is practically equal to the bare Coulomb force, indicating that most of the electronic density has been pushed out of the inter-bond region. Subsequently the laser intensity dies off as the electric field changes its sign and some electronic density returns to screen and weaken the bare Coulomb force. By the time the nuclei reach a distance of $3.2a_0$, the probability of electrons being in the bond region is zero (ionization complete) and the force is purely a Coulomb repulsion.

We plot the distance between the two D nuclei as a function of time in Figure 2b. It is seen that the distance grows monotonically with time. Initially the growth is slow. After about 5 fs the appreciable ionization sets in and detonates the explosive nature of the process Ionization is more or less complete at $t =$ 9 fs, i.e., when the nuclei are at a distance of $R \approx 2.6a_0$.

A useful way to determine the final kinetic energy is to evaluate the "effective energy" of the exploding nuclei

$$E_{eff} = \frac{1}{2}\mu\dot{R}^2 + \frac{1}{R}, \tag{3.2}$$

where μ is the reduced mass $M/2$. E_{eff} converges to the final kinetic energy much faster than the bare kinetic energy. This is seen in Figure 2c, where $E_{eff}/2$ (the average energy per nucleus) is practically converged to the final kinetic energy per D value of 7.6 eV at $t \approx 8$ fs, close to the completion of ionization.

Since the molecule is symmetrical and initially neutral, the kinetic energy of the center of mass (CM) motion is small when compared to the relative kinetic energy. In Figure 2d, we show the temporal CM kinetic energy. Up to $t = 5$ fs there is almost no interaction between the center of mass and the electric field, because the molecule is by large neutral. Subsequently, ionization sets in and the center of mass is affected by the laser field, experiencing oscillatory kicks. As the pulse dies out, the remaining CM kinetic energy is basically zero, thus not contributing in any essential way to the kinetic energy of the ionic fragments.

B. The D^+ Kinetic Energy Distribution. In the previous subsection, we described in some detail the Coulomb explosion of an archetype case. To compare to experiment, we need to perform additional runs, sampling the quantum nature of the initial vibrational state (we assume the D_2 molecule is in its vibrational ground-state prior to the pulse). Assuming the nuclei explode along their molecular axis, the polarization axis angle

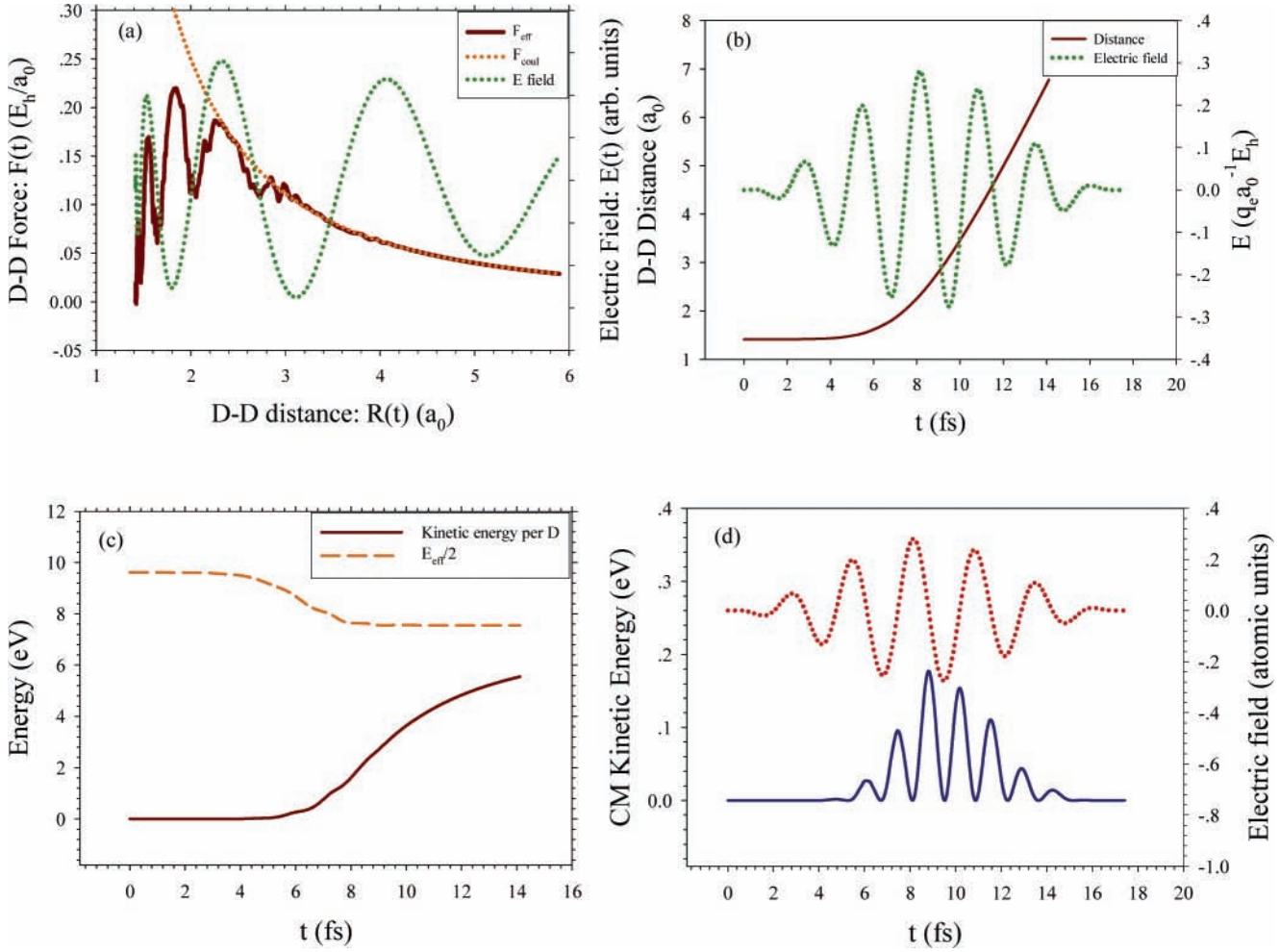

Figure 2. (a) Effective force and bare Coulomb force between the nuclei as a function of their distance $R(t)$. (b) D−D bond length as a function of time. (c) Kinetic energy and E_{eff} per D nucleus as a function of time for the archetype run. (d) Center of mass kinetic energy (solid line) of the D_2 molecule as a function of time for the archetype run. Also shown, the electric field (dotted). All results refer to the archetypal run. In runs a, b, and d, the external electric field is superimposed as well.

is determined in experiment by adjusting the angle between polarization and mass-spectrometer. The effect of initial bond length and initial momentum on the final D^+ kinetic energy is shown in Figure 3a. The results are surprising. The most evident feature is that the final kinetic energy becomes smaller when the bond length is shortened. Intuition would have it that if the nuclei are closer, the final kinetic energy should be larger. If ionization was extremely fast, then the final kinetic energy per D^+ when the bond length is $1.1a_0$ would be 12.4 eV, while for a bond length of $1.42a_0$ it is 9.6 eV. A plausible explanation for the behavior seen in Figure 3a is that the ionization rate is greatly reduced when the bond length is smaller. However, as seen in Figure 3b this cannot be: exactly the opposite happens! The ionization rate when the bond is compressed is noticeably larger. Something else is happening. The puzzle is solved by noticing that ionization does not start promptly when the pulse is turned on. Because it takes time for the field to reach a high value, ionization starts only 4 fs after the pulse is turned on. During this time, the compressed bond, starting at $R_0 = 1.1a_0$ has time to relax and even stretch. This can be seen in Figure 3c. By the time ionization starts at 4 fs, the compressed bond length has become a stretched bond length at an extension of $1.8a_0$. This accounts for the fact that the compressed bond yields smaller kinetic energy. During the explosion, the ionization as a function of the instantaneous bond length is shown in Figure 3d for the two initial bond lengths. It is seen that the ionization is higher at small bond lengths for the $R_0 = 1.42a_0$ trajectory, when compared to that starting at $R_0 = 1.12a_0$. This is the cause for the higher final kinetic energy.

The kinetic energy distribution is obtained by selecting the initial conditions at random from the Wigner distribution corresponding to the $v = 0$ vibrational D_2 wave function. We assume the wave function is a Gaussian $\psi(R) \propto \exp[-(1/2\sigma^2)-(R - R_0)^2]$, with $R_0 = 1.42a_0$ and $\sigma = 0.189a_0$, these parameters are a fit to the vibrational wave packet of the D_2 potential curve calculated using the LDA functional.

C. Effect of Orientation and Rotation. The experimental setup[33] is such that (ideally) only molecules aligned with the field polarization direction make it to the detectors. Of course, a small deviance from this is possible, however, and we have made simulations to ensure that the results presented above do not change appreciably when the angle between the molecular axis and the polarization changes a little.

Besides orientation, there may also be an effect of rotational motion during the explosion. However, this is negligible, as we now explain. First, we note that the rotational temperature of the molecules in the molecular beam can be estimated to be[77,78] ~100 K. Given the relatively low mass of deuterium, this means that the angular momentum of the molecule is low: the probability is negligible for $l \geq 3$, where l is the rotational quantum number. Now, to estimate the effect of angular momentum, we stipulate the relation $\hbar l \approx M_I R(t)^2 \dot{\theta}(t)$ where θ is the angle between the molecular axis and the electric field polaization. The total change in direction of the projectile is

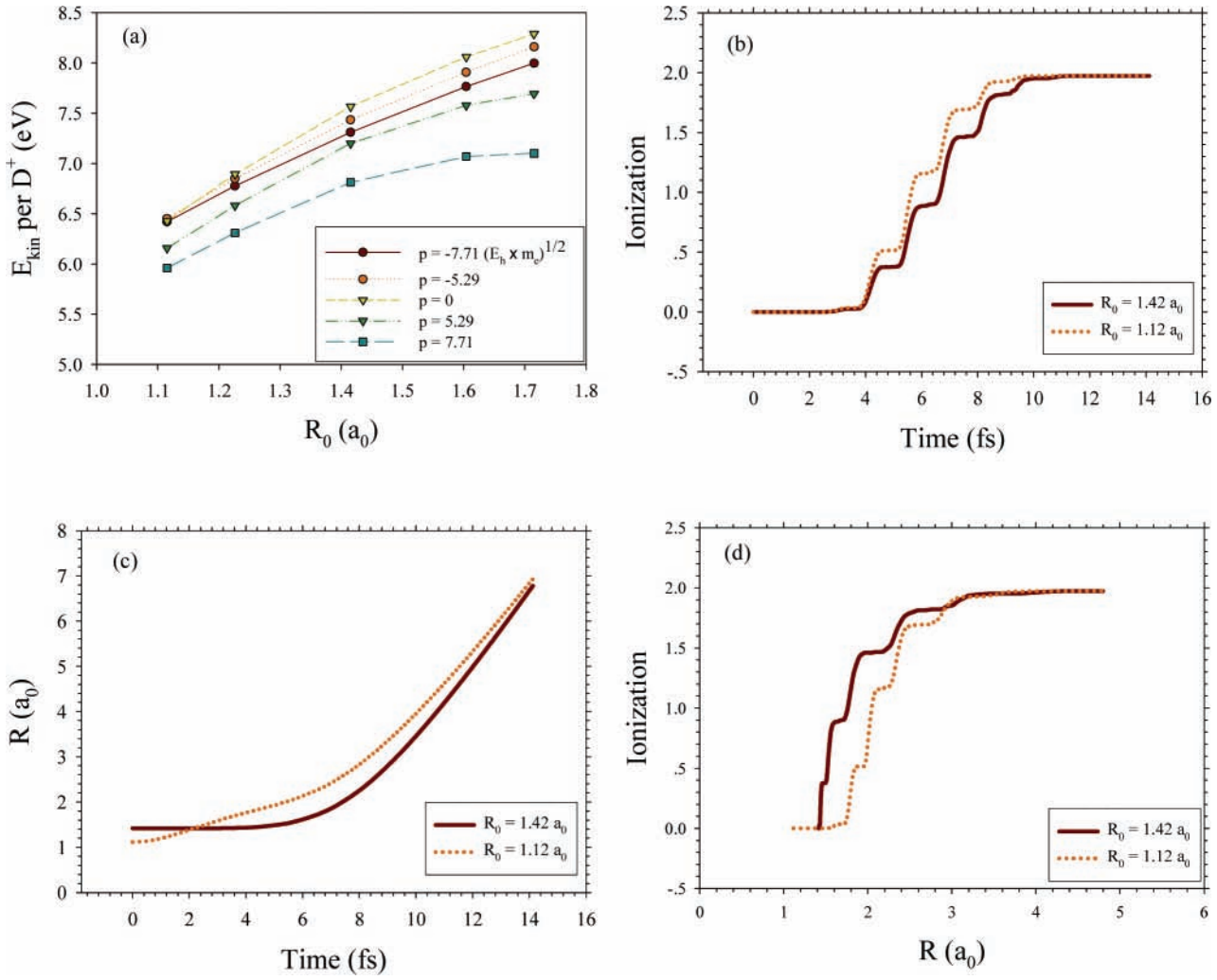

Figure 3. (a) KE distribution of the D^+ vs initial bond length and momentum. (b) Ionization as a function of time for the two initial bond lengths of $1.42a_0$ and $1.12a_0$ (zero initial momentum). (c) Distance between the D nuclei as a function of time at different initial positions. (d) Ionization as a function of time for the two initial bond lengths of $1.42a_0$ and $1.12a_0$. All results shown use ALDA.

therefore: $\Delta\theta \approx l \int_0^\infty (\hbar dt/M_I R(t)^2)$. The integral can be estimated from our quantum simulation and is on the order of 0.07. Thus, the probable change in θ is 0.07 and the largest change is 0.14. Since $\cos[0.14] = 0.99$, we estimate that the rotational effects can change the results by only a few percent. During the short pulse, there is not enough time for any angular change.

IV. Other TDDFT Functionals

To check the sensitivity of the results to the underlying electron dynamics theory, we performed a time-dependent Hartree−Fock (TDHF) simulation of the Coulomb explosion. TDHF in the case of D_2 is a time-dependent density functional. TDHF does not suffer from self-interaction (most notably, self-repulsion) effects, as does the TD-ALDA. However, TDHF does not account for electron correlation. We have also studied the new functional[48] we term the ABN1 functional described in detail in section 2. This functional enjoys the benefit of including correlation effects (somewhat similar to the ALDA) while on the other hand not suffering from long-range self-repulsion.

The resulting distributions using TDLDA, TDHF, and the ABN1 functional are shown in Figure 4, compared with the measured curve[33] (all distribution curves are normalized). The theoretical curves are all similar in shape but much narrower than the experiment.

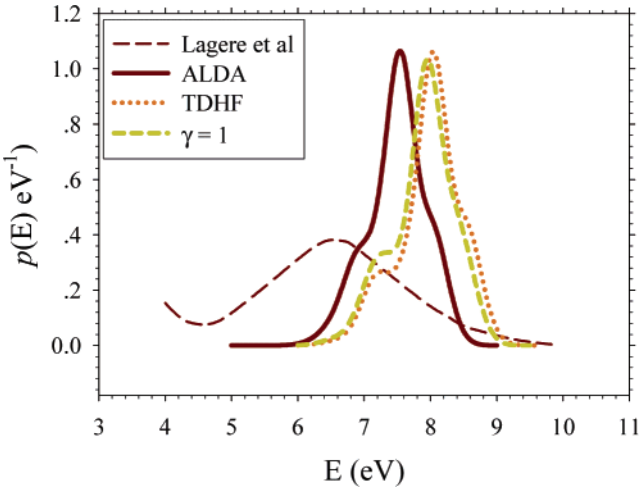

Figure 4. Kinetic energy distribution: experiment[33] (dashed) and calculated, based on TD-ALDA (solid), TD-HF (dotted) and the TD-ABN1 functional.

The experimental most probable kinetic energy is ~6.5 eV. Of the three theoretical variants, the closest is the TD-ALDA curve. It peak at 7.5 eV, a significant deviation. The TDHF and the ABN1 functional give almost identical results, peaking at ~8 eV. This is somewhat surprising, since the ABN1 functional enjoys the correlation effects similar to TDALDA

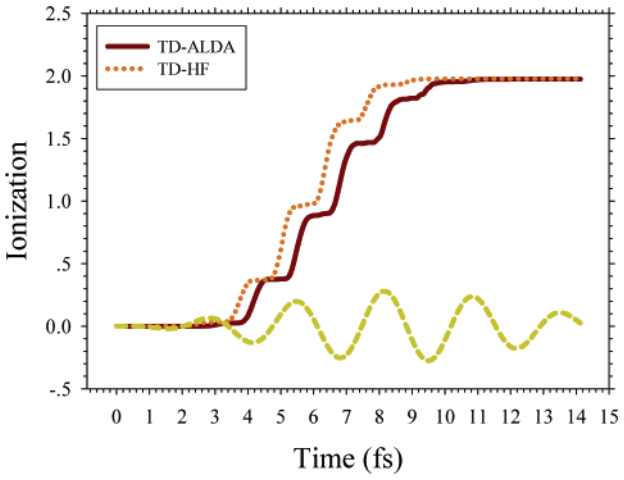

Figure 5. Time schedule of ionization. TD-ALDA (solid) vs TDHF (dotted) results. The field strength (dashed) is also given.

while not including self-repulsion. The conclusion we must draw is that the TD-ALDA enjoys an error cancellation effect which is disturbed when it is corrected for self-repulsion. TDHF calculated final kinetic energy peaks too high relative to TDLDA calculations because it predicts too high ionization rates. In Figure 5, we find that in TDHF complete ionization is achieved ~1.5 fs before it is achieved in TD-ALDA. Thus, the deuterium nuclei are exposed unscreened by the electrons when they are closer, resulting in a more violent explosion.

V. Discussion

In this paper, we have presented several ab initio simulations of recent Coulomb explosion experiments on the D_2 molecule. Using the simulations, we can study the (classical) dynamics of the nuclei as well as the dynamics of the electrons. We find that these are intricately entangled, since although the laser pulses are very short, the nuclei move considerably during the pulse and such motion must be properly taken into account when trying to reconstruct, for example, the nuclear position before the pulse is given.

An interesting consequence of this study is that the D^+ kinetic energy distribution is very sensitive to the underlying TDDFT functional. This shows that such experiments can form additional benchmark systems for the development of future TDDFT functionals.

An important conclusion from the present calculations is that the combination of Ehrenfest molecular dynamics and the widely used ALDA functional cannot properly account for the observed results. A recent paper[13] discusses the shortcomings of ALDA alone for describing the single and double ionization rates in He atom. We have also tested the recently developed ABN1 functional, which fixes several formal shortcomings of the LDA functional while still taking correlation effects into account. Combining it with molecular dynamics, it too was found unsatisfactory, showing similar results to the TDHF calculation. We concluded that in ALDA there probably exists a delicate cancellation of errors, so that when self-repulsion is removed, the overall performance of ALDA is less satisfactory.

Another noticeable fact is that all calculated results showed much too narrow kinetic energy distributions. The experimental distribution[33] is not only wider but also rises toward low kinetic energies (lower than 4.5 eV). This effect is not seen in the theoretical calculation. The most probable kinetic energy was found in calculation, when compared with experiment, to be 1 eV too high (ALDA) and 1.5 eV too high (BN1 and TDHF). One possible cause for the poor correspondence with experiment is that the TDDFT functionals lead to exaggerated large ionization rate exposing the nuclei to the bare Coulomb repulsion too early. It has been established that electron correlation should be described with "memory functionals" within a current density functional theory.[59−62,79,80] In the linear response regime, the memory effects introduce some viscosity-like behavior for the electron "fluid" dynamics. Such an effect may decrease the ionization rate, however to date there is no available memory functional suitable for nonlinear-response dynamics. The need for memory functionals results from the steplike dependence of the ionization process on the nuclear separation. This results in sudden rapid ionization which cannot be described properly by adiabatic functionals.

The small width of the distributions may also be a result of the use of classical Ehrenfest molecular dynamics. The theoretical simulations of Legaré et al.,[33] using a wave packet to describe nuclear dynamics also showed a narrow distribution, but these calculations are probably more appropriate for weaker fields than considered here since they assume sequential ionization. We are currently developing a new real-time first-principles approach to describe combined electron−nuclear dynamics where nuclei are treated quantum mechanically using a derivative of a recent general theory,[81] combined with a TDDFT simulation.

An additional venue for future work is to study the Coulomb explosion processes in larger molecules. Such systems include a larger number of electrons and it will be interesting to compare theory to new experimental results[32] in order to study the performance of TDDFT functionals.

Acknowledgment. This research was supported by the German Israel Foundation. The authors wish to thank Profs. Sandy Ruhman and Ronnie Kosloff for their support, critical comments and enlightening discussions. We also thank Prof. U. Even for his help in estimating the molecular beam rotational temperature.

References and Notes

(1) Runge, E.; Gross, E. K. U. *Phys. Rev. Lett.* **1984**, *52*, 997.
(2) Baer, R. *Chem. Phys. Lett.* **2002**, *364*, 75.
(3) Bauernschmitt, R.; Ahlrichs, R. *Chem. Phys. Lett.* **1996**, *256* (4−5), 454.
(4) Bauernschmitt, R.; Ahlrichs, R.; Hennrich, F. H.; Kappes, M. M. *J. Am. Chem. Soc.* **1998**, *120*, 5052.
(5) Gross, E. K. U.; Dobson, J. F.; Petersilka, M. In *Density Functional Theory II: Relativistic and Time Dependent Extensions*; Nalewajski, R. F., Ed.; Springer: New York, 1996; p 81.
(6) Stener, M.; Fronzoni, G.; Toffoli, D.; Decleva, P. *Chem. Phys.* **2002**, *282* (3), 337.
(7) Baer, R.; Neuhauser, D.; Zdanska, P.; Moiseyev, N. *Phys. Rev. A* **2003**, *68* (4), 043406.
(8) Hirata, S.; Head-Gordon, M. *Chem. Phys. Lett.* **1999**, *314* (3−4), 291.
(9) Dreuw, A.; Weisman, J. L.; Head-Gordon, M. *J. Chem. Phys.* **2003**, *119*, 2943.
(10) Bertsch, G. F.; Schnell, A.; Yabana, K. *J. Chem. Phys.* **2001**, *115*, 4051.
(11) Yabana, K.; Bertsch, G. F. *Czech. J. Phys.* **1998**, *48* (6−7), 760.
(12) Marques, M. A. L.; Castro, A.; Bertsch, G. F.; Rubio, A. *Comput. Phys. Comm.* **2003**, *151* (1), 60.
(13) Petersilka, M.; Gross, E. K. U. *Laser Phys.* **1999**, *9* (1), 105.
(14) Maitra, N. T.; Burke, K.; Appel, H.; Gross, E. K. U.; van Leeuwen, R. *Reviews in Modern Quantum Chemsitry: A celebration of the contributions of R. G. Parr*; World-Scientific: Singapore, 2002.
(15) Stratmann, R. E.; Scuseria, G. E.; Frisch, M. J. *J. Chem. Phys.* **1998**, 109, 8218.
(16) van Leeuwen, R. *Phys. Rev. Lett.* **1998**, *80*, 1280.
(17) Kohn, W.; Meir, Y.; Makarov, D. E. *Phys. Rev. Lett.* **1998**, 80, 4153.

(18) Ullrich, C. A.; Reinhard, P. G.; Suraud, E. *J. Phys. B* **1998**, *31*, 1871.
(19) Ullrich, C. A.; Vignale, G. *Phys. Rev. B* **2002**, *65*, 245102.
(20) Baer, R.; Kurzweil, Y.; Cederbaum, L. S. *Isr. J. Chem.* **2005**, *45* (1−2), 161.
(21) Kallush, S.; Band, Y.; Baer, R. *Chem. Phys. Lett.* **2004**, *392*, 23.
(22) Hawthorne, M. F.; Zink, J. I.; Skelton, J. M.; Bayer, M. J.; Liu, C.; Livshits, E.; Baer, R.; Neuhauser, D. *Science* **2004**, *303* (5665), 1849.
(23) Baer, R.; Neuhasuer, D. *J. Chem. Phys.* **2004**, *121*, 9803.
(24) Chelikowsky, J. R.; Kronik, L.; Vasiliev, I. *J. Phys. C* **2003**, *15*, R1517.
(25) Burke, K.; Werschnik, J.; Gross, E. K. U. *J. Chem. Phys.* **2005**, *123*, 062206.
(26) Appel, H.; Gross, E. K. U.; Burke, K. *Phys. Rev. Lett.* **2003**, *90*, 043005.
(27) Ullrich, C. A.; Burke, K. *J. Chem. Phys.* **2004**, *121* (1), 28.
(28) Sottile, F.; Bruneval, F.; Marinopoulos, A. G.; Dash, L. K.; Botti, S.; Olevano, V.; Vast, N.; Rubio, A.; Reining, L. *Int. J. Quantum Chem.* **2005**, *102*, 684.
(29) Castro, A.; Marques, M. A. L.; Alonso, J. A.; Bertsch, G. F.; Rubio, A. *Eur. Phys. J. D* **2004**, *28* (2), 211.
(30) Marx, D.; Hutter, J. In *Modern Methods and Algorithms of Quantum Chemistry, Proceedings*; Grotendorst, J., Ed.; John von Neumann Institute for Computing: Julich, Germany, 2000; Vol. 3, p 329.
(31) Baer, R.; Siam, N. *J. Chem. Phys.* **2004**, *121*, 6341.
(32) Legare, F.; Lee, K. F.; Litvinyuk, I. V.; Dooley, P. W.; Wesolowski, S. S.; Bunker, P. R.; Dombi, P.; Krausz, F.; Bandrauk, A. D.; Villeneuve, D. M.; Corkum, P. B. *Phys. Rev. A* **2005**, *71* (1).
(33) Legare, F.; Litvinyuk, I. V.; Dooley, P. W.; Quere, F.; Bandrauk, A. D.; Villeneuve, D. M.; Corkum, P. B. *Phys. Rev. Lett.* **2003**, *91*, 093002.
(34) Rudenko, A.; Feuerstein, B.; Zrost, K.; de Jesus, V. L. B.; Ergler, T.; Dimopoulou, C.; Schroter, C. D.; Moshammer, R.; Ullrich, J. *J. Phys. B* **2005**, *38*, 487.
(35) Shimizu, S.; Zhakhovskii, V.; Murakami, M.; Tanaka, M.; Yatsuhashi, T.; Okihara, S.; Nishihara, K.; Sakabe, S.; Izawa, Y.; Nakashima, N. *Chem. Phys. Lett.* **2005**, *404* (4−6), 379.
(36) Ma, R.; Li, X.; Ren, H. Z.; Yang, H.; Jiang, H. B.; Gong, Q. H. *Int. J. Mass Spectrom.* **2005**, *242* (1), 43.
(37) Posthumus, J. H. *Rep. Prog. Phys.* **2004**, *67*, 623.
(38) Markevitch, A. N.; Romanov, D. A.; Smith, S. M.; Levis, R. *J. Phys. Rev. Lett.* **2004**, *92* (6).
(39) Last, I.; Jortner, J. *J. Chem. Phys.* **2004**, *121*, 3030.
(40) Zweiback, J.; Smith, R. A.; Cowan, T. E.; Hays, G.; Wharton, K. B.; Yanovsky, V. P.; Ditmire, T. *Phys. Rev. Lett.* **2000**, *84*, 2634.
(41) Lein, M.; Kreibich, T.; Gross, E. K. U.; Engel, V. *Phys. Rev. A* **2002**, *65*, 033403.
(42) Walker, B.; Sheehy, B.; Dimauro, L. F.; Agostini, P.; Schafer, K. J.; Kulander, K. C. *Phys. Rev. Lett.* **1994**, *73*, 1227.
(43) Chelkowski, S.; Corkum, P. B.; Bandrauk, A. D. *Phys. Rev. Lett.* **1999**, 82, 3416.
(44) Lein, M.; Kummel, S. *Phys. Rev. Lett.* **2005**, *94*, 143003.
(45) Perdew, J. P.; Levy, M. *Phys. Rev. Lett.* **1983**, *51*, 1884.
(46) Fittinghoff, D. N.; Bolton, P. R.; Chang, B.; Kulander, K. C. *Phys. Rev. Lett.* **1992**, *69*, 2642.
(47) Lappas, D. G.; van Leeuwen, R. *J. Phys. B* **1998**, *31*, L249.
(48) Baer, R.; Neuhauser, D. *Phys. Rev. Lett.* **2005**, *94*, 043002.
(49) Kohn, W.; Sham, L. J. *Phys. Rev.* **1965**, *140*, A1133.
(50) Gunnarsson, O.; Lundqvist, B. I. *Phys. Rev. B* **1976**, *13*, 4274.
(51) Perdew, J. P.; Wang, Y. *Phys. Rev. B* **1992**, *45*, 13244.
(52) Ehrenfest, P. *Z. Phys.* **1927**, *45*.
(53) Theilhaber, J. *Phys. Rev. B* **1992**, *46*, 12990.
(54) Baer, R.; Weiss, S.; Neuhauser, D. *Nano Lett.* **2004**, *4*, 85.
(55) Baer, R.; Seideman, T.; Ilani, S.; Neuhauser, D. *J. Chem. Phys.* **2003**, *120*, 3387.
(56) Baer, R.; Gould, R. *J. Chem. Phys.* **2001**, *114* (8), 3385.
(57) Baer, R.; Neuhauser, D. *Int. J. Quantum Chem.* **2003**, *91* (3), 524.
(58) It is important to distinguish between the nonadiabatic effects of the nuclear motion (with respect to the Born−Oppenheimer approximation) and the nonadiabatic approximation in the exchange-correlation potentials.
(59) Kurzweil, Y.; Baer, R. *J. Chem. Phys.* **2004**, *121*, 8731.
(60) Kurzweil, Y.; Baer, R. *Phys. Rev. B* **2005**, *72*, 035106.
(61) Dobson, J. F.; Bunner, M. J.; Gross, E. K. U. *Phys. Rev. Lett.* **1997**, *79*, 1905.
(62) Kurzweil, Y.; Baer, R. *Phys. Rev. B* **2005**, in press.
(63) Uhlmann, M.; Kunert, T.; Grossmann, F.; Schmidt, R. *Phys. Rev. A* **2003**, *67*, 013413.
(64) Chelkowski, S.; Zuo, T.; Atabek, O.; Bandrauk, A. D. *Phys. Rev. A* **1995**, *52*, 2977.
(65) Perdew, J. P.; Parr, R. G.; Levy, M.; Balduz, J. L. *Phys. Rev. Lett.* **1982**, *49*, 1691.
(66) Wigner, E. *Phys. Rev.* **1934**, *46*, 1002.
(67) Rassolov, V. A.; Pople, J. A.; Ratner, M. A. *Phys. Rev. B* **1999**, *59*, 15625.
(68) Robinson, J. E.; Bassani, F.; Knox, R. S.; Schreiffer, J. R. *Phys. Rev. Lett.* **1962**, *9*, 215.
(69) Baer, R.; Neuhasuer, D. Manuscript in preparation 2005.
(70) Payne, M. C.; Teter, M. P.; Allan, D. C.; Arias, T. A.; Joannopoulos, J. D. *Rev. Mod. Phys.* **1992**, *64*, 1045.
(71) Martyna, G. J.; Tuckerman, M. E. *J. Chem. Phys.* **1999**, *110*, 2810.
(72) Troullier, N.; Martins, J. L. *Phys. Rev. B* **1991**, *43*, 1993.
(73) Since we are working within LSDA, we are in fact allowing spin relaxation, by decoupling the up and down spin densities.
(74) Press, W. H.; Teukolsky, S. A.; Vetterling, W. T.; Flannery, B. P. *Numerical Recipes in C*; Cambridge University Press: Cambridge, U.K., 1992.
(75) Neuhasuer, D.; Baer, M. *J. Chem. Phys.* **1989**, *90*, 4351.
(76) Bucksbaum, P. H.; Zavriyev, A.; Muller, H. G.; Schumacher, D. W. *Phys. Rev. Lett.* **1990**, *64*, 1883.
(77) Hillenkamp, M.; Keinan, S.; Even, U. *J. Chem. Phys.* **2003**, *118*, 8699.
(78) Even, U. private communication.
(79) Gross, E. K. U.; Kohn, W. *Phys. Rev. Lett.* **1985**, *55*, 2850.
(80) Vignale, G.; Kohn, W. *Phys. Rev. Lett.* **1996**, *77*, 2037.
(81) Baer, R.; Kouri, D. J.; Baer, M.; Hoffman, D. K. *J. Chem. Phys.* **2003**, *119*, 6998.